

# Crystallization of FeC Iron Monocarbide During Peritectoidal Transformation of the Lamellar Eutectoid of Ledeburite White Eutectic Cast Iron



Sergey Vasilyevich Davydov<sup>1,\*</sup>

*1 Bryansk State Technical University, Russia*

\*Corresponding author: Sergey Vasilyevich Davydov, Bryansk State Technical University, Russia. Email: [fulleren\\_grafen@mail.ru](mailto:fulleren_grafen@mail.ru)

**Abstract:** The previously unknown process of homogeneous and heterogeneous crystallization of FeC iron monocarbide and its co-crystallizations with  $\epsilon$ -carbide  $\text{Fe}_2\text{C}$  from a supersaturated solid solution based on  $\epsilon$ -carbide  $\text{Fe}_2\text{C}$  or polycarbide quasi-eutectic formed in the process of peritectoid decomposition during prolonged heating (isothermal annealing) of the lamellar eutectoid ledeburite in cast eutectic white iron has been investigated. Crystallization of 2D monolayers of FeC monocarbide allotropes in the form of translucent extended and elastic crystalline nanofilms has been experimentally proved. The carbide phases in white cast iron can be characterized as a single isomorphous and isostructural quasi-carbide solid solution, which structurally crystallizes as a mixture of carbide phases as a quasi-eutectic, in which the carbon content is free to vary widely without identification of the carbide phases proper. The decomposition product of the lamellar eutectoid as a result of peritectoid transformation during isothermal annealing is polycarbide with a gradient crystal lattice of solid solutions corresponding in carbon concentration to this or that carbide.

**Keywords:** lamellar eutectoid, troostite, crystallizations, polycarbide

## 1. Introduction

There are no objective data on FeC monocarbide as a chemical compound [1,2]. FeC monocarbide has not been systematically investigated and is not mentioned either in works on the Fe-C diagram or in general in materials science and metallurgy [3,4]. In the work of M. Bahgat [5] discusses various methods (gaseous carburization, mechanochemical synthesis, laser pyrolysis, plasma pyrolysis, chemical vapor deposition, ion implantation) for the synthesis of basic iron carbides ( $\text{Fe}_3\text{C}$ ,  $\text{Fe}_7\text{C}_3$ ,  $\text{Fe}_5\text{C}_2$ ,  $\text{Fe}_2\text{C}$ ); attention is also paid to the exotic carbide  $\text{Fe}_{75}\text{C}_{25}$ , but the synthesis of FeC iron monocarbide is not considered.

Comprehensive studies of FeC monocarbide began in a scientific discipline that has nothing to do with materials science and metallurgy - astrophysics. In the spectra of star formation and cold carbon stars in 1988, lines of FeC monocarbide and monocarbides of other elements, such as SiC, were detected. This fact was the impetus for investigating, first of all, the spectral characteristics of the FeC monocarbide molecule and its atomic and electronic structure. However, these studies had to be postponed

because it was impossible to obtain FeC monocarbide by existing chemical and metallurgical technologies, and it was necessary to develop fundamentally new technologies for the synthesis of FeC monocarbide only in the form of single molecules.

The first studies of spectroscopic characteristics of FeC monocarbide molecules by resonant two-photon ionisation spectroscopy were performed by W. J. Balfour [6]. J. Balfour [6], in which FeC monocarbide was obtained as a result of the reaction of laser-vaporised iron atoms with methane in a helium atmosphere at its supersonic expansion. The electronic structure of FeC monocarbide was investigated by Shim I [7]. In this work, the dissociation energy  $D_e$  of FeC monocarbide was determined to be 2.79 eV. In the work of Dale J. Brugh [8], FeC monocarbide was studied by resonant two-photon ionization spectroscopy and some new electronic states were identified, and the binding energy was determined to be  $3.9 \pm 0.3$  eV and the ionisation energy to be  $7.74 \pm 0.09$  eV.

To obtain FeC monocarbide, Dale J. Brugh [8] applied a rather complex and virtuoso technology. Initially, the production of FeC monocarbide was achieved by pulsed

laser ablation of a carbon steel target disc with a power of 1 to 2 mJ of the second harmonic of the Nd:YAG laser in a supersonic expansion beam of 3% methane in helium, which after passing through a 3 cm channel was expanded through a 2 mm diameter hole. The mole percentage of carbon in the carbon steel sample disc was too low to produce appreciable amounts of FeC molecules in the pure helium expansion. Replacing the disc with a sample pressed from a powder consisting of iron and carbon powders in a molar ratio of 3:1 was about twice as efficient for FeC production as the carbon steel method.

In the studies of Aiuchi K. [9], FeC monocarbide was obtained by laser ablation reaction of Fe atoms with CH<sub>4</sub> methane, and its spectrum was studied using laser-induced fluorescence. In the visible region of the spectrum it was possible to characterize five electronic states and investigate spin-orbit splitting. Spin analysis was performed for 46 vibronic bands. Thirty-five bands were observed for the first time.

The permanent electric dipole moments of FeC monocarbide were investigated by Timothy C. Steimle [10]. For the first time in the laboratory using direct absorption techniques in the millimetre-submillimetre range Allen M. D. [11] measured the pure rotational spectrum and investigated some spin-orbit parameters of FeC monocarbide, which was synthesized as a result of the reaction of iron vapor produced in a high-temperature Broyde-type furnace in an atmosphere of methane gas under DC discharge conditions.

The studies of FeC monocarbide, the results of which are applicable in metallurgy for the analysis of phase processes and structure formation in the Fe-Fe<sub>3</sub>C system, have been performed relatively recently in 2016-2022 [12-15]. In these and other works, it was found that FeC monocarbide has unique properties such as superconductivity, metallic and catalytic properties in the synthesis of carbon nanotubes and in Fischer-Tropsch liquid fuel synthesis (FTS). It was found that the structure of FeC monocarbide is layered and has enormous internal capacitance, for example, for lithium atoms, which makes it possible to use FeC monocarbide as a basis in rechargeable lithium batteries.

In Liu, X. W. [12] was the first to perform Mössbauer spectroscopy of iron carbides ( $\alpha$ -Fe,  $\gamma'$ -FeC,  $\eta$ -Fe<sub>2</sub>C,  $\zeta$ -Fe<sub>2</sub>C,  $\chi$ -Fe<sub>5</sub>C<sub>2</sub>, h-Fe<sub>7</sub>C<sub>3</sub>,  $\theta$ -Fe<sub>3</sub>C, o-Fe<sub>7</sub>C<sub>3</sub>,  $\gamma'$ -Fe<sub>4</sub>C,  $\gamma''$ -Fe<sub>4</sub>C and  $\alpha'$ -Fe<sub>16</sub>C<sub>2</sub>) using the full-potential linearised plane wave method, which enabled the determination of the crystallographic structure of the whole line of carbides. The Mössbauer parameters of  $\gamma'$ -FeC,  $\eta$ -Fe<sub>2</sub>C,  $\zeta$ -Fe<sub>2</sub>C, h-Fe<sub>7</sub>C<sub>3</sub>, o-Fe<sub>7</sub>C<sub>3</sub>,  $\gamma'$ -Fe<sub>4</sub>C,  $\gamma''$ -Fe<sub>4</sub>C and  $\alpha'$ -Fe<sub>16</sub>C<sub>2</sub> have also been theoretically predicted. Almost single-phase  $\chi$ -Fe<sub>5</sub>C<sub>2</sub> and  $\theta$ -Fe<sub>3</sub>C were experimentally obtained.

Mössbauer spectroscopy of iron carbides revealed the crystallographic correspondence of the carbide structures and their stability. Depending on the places occupied by carbon atoms in the carbide crystal lattice, all these carbides can be divided into octahedral, trigonal-prismatic and tetrahedral [12].

The octahedral carbides include  $\gamma'$ -FeC,  $\alpha'$ -Fe<sub>16</sub>C<sub>2</sub>,  $\eta$ -Fe<sub>2</sub>C,  $\zeta$ -Fe<sub>2</sub>C and  $\gamma''$ -Fe<sub>4</sub>C carbides. In addition,  $\gamma'$ -FeC and  $\gamma''$ -Fe<sub>4</sub>C consist of  $\gamma$ -Fe (HCC) sublattices with octahedral

interdoped C atoms. The  $\eta$ -Fe<sub>2</sub>C and  $\zeta$ -Fe<sub>2</sub>C carbides have hexagonal dense packing of Fe sublattices.

The second type of carbides are trigonal-prismatic carbides h-Fe<sub>7</sub>C<sub>3</sub>, o-Fe<sub>7</sub>C<sub>3</sub>,  $\chi$ -Fe<sub>5</sub>C<sub>2</sub> and  $\theta$ -Fe<sub>3</sub>C, in which C atoms are arranged in trigonal-prismatic sites of distorted hexagonal-closed structure of Fe atoms. The last type is the tetrahedral carbide,  $\gamma'$ -Fe<sub>4</sub>C.

The average distance between Fe and C atoms in these carbides is about 1.90 Å, which falls within the expected range of Fe-C distances for many carbide structures. The closest distance between C and C atoms varies from 2.60 Å to 3.50 Å, indicating the absence of C-C dimers in the iron carbides.

The studies [12-15] provide, to a fairly certain extent, an opportunity to further explain many important points, including the high variable percentage of carbon content in the carbide phases.

Dong F [13,14] have performed theoretical studies of the crystallographic structure of FeC monocarbide and its some thermodynamic properties for the first time, and mechanical properties have been calculated. Dong F [13,14] by ab initio simulations (VASP) theoretically discovered energetically stable two-dimensional allotropes of FeC monocarbide characterized by planar hypercoordination chemical bonding, respectively: tetragonal FeC monocarbide (t-FeC) and orthorhombic FeC monocarbide (o-FeC).

From an energetic point of view, the t-FeC allotrope is a two-dimensional tetragonal layer in which each carbon atom is four-coordinated with the surrounding four iron atoms. The o-FeC allotrope monolayer is an orthorhombic planar phase with a pentacoordinated carbon bond and a planar seven-coordinated bond of iron atoms. The FeC monocarbide allotropes are the first example of 2D monolayers with simultaneously pentacoordinated carbon bonds and semi-coordinated iron atom bonds in known iron-carbon materials. Theoretical calculations confirm that all these monolayers have significant dynamic, mechanical and thermal stability.

Dong F [13,14] calculated the Ecoh cohesive energies of t-FeC and o-FeC allotrope monolayers to be 5.76 and 5.59 eV/atom, respectively. The high cohesive energy is a guarantee that t-FeC and o-FeC monolayers are strongly bonded iron-carbon networks. The structure of the t-FeC monolayer can be regarded as a quasi-planar tetragonal lattice with space group P4/nmm, in which each C atom is quasi-planarly four-coordinated with the surrounding four Fe atoms. The planar monolayer of the t-FeC allotrope has a slightly corrugated square structure with a thickness of  $\delta=1.26$  Å. The lattice constants are  $a=b=3.49$  Å.

The structure of the o-FeC monolayer can be regarded as a quasi-planar orthorhombic lattice with space group Cmmm, in which each C atom is quasi-planarly coordinated with five neighboring atoms (one C atom and four Fe atoms), forming a planar five-coordinate bond, and each Fe atom is coordinated with four carbon atoms and three iron atoms, forming a planar seven-coordinate bond. Therefore, unlike the t-FeC monolayer with a corrugated structure, the o-FeC monolayer has a perfect flat lattice with thickness  $\delta=1.85$  Å. The lattice constants are  $a=5.96$

$\text{\AA}$ ,  $b = 4.49 \text{ \AA}$ . This type of bonding in the monolayers of o-FeC and t-FeC allotropes determines its metallic character.

In the thesis work of the Russian scientist K.V.Larionov [15], FeC monocarbide and its allotropes o-FeC and t-FeC were also studied. The energetic favorability of the layered orthorhombic phase of FeC monocarbide was shown and the thermodynamic stability of the orthorhombic monolayers of the o-FeC allotrope and the corrugated monolayers of the t-FeC allotrope phase was proved.

It is possible to obtain monophase FeC monocarbide, as well as other iron carbides, from ledeburite two-component (Fe+C) white cast irons of eutectic and transeutectic composition in accordance with the diagram of state of Fe-C alloys, but this issue of research of FeC monocarbide isolated from white cast irons has not been considered so far even in theoretical terms.

Ledeburite of white cast iron or eutectic of two-component Fe-C alloy is traditionally known as a stable two-phase structure (cementite+ferrite) of white eutectic cast irrespective of their chemical composition [16-18] and is thermodynamically relatively stable to external thermal effects, except for the production of ductile cast iron [19, 20].

Recently, ledeburite has been considered either as an intermetallic compound in the structure of iron-carbon alloys, for example, as a steel of the ledeburite class in the production of Damascus steel [21], or as a natural metal-ceramic composite material. Vasyunina N. V. showed [22] that according to the results of X-ray diffraction analysis, the structure of cast iron containing 93.8%Fe and 4.99 %C is considered as hypereutectic white cast iron with a composite structure (ledeburite + graphite).

The production of iron carbides is also possible during the heat treatment of ledeburite, as well as quenching martensite. If, during prolonged high-temperature graphitizing annealing, cementite and ledeburite of white cast iron completely decomposes into perlite and floccular graphite, with the formation of a ductile iron structure [19, 20], then during controlled annealing, ledeburite decomposes into carbides.

Sukhanov D.A. established [23] that in the process of isothermal annealing of high-purity two-component white cast iron (2.25%C) at 650-950°C, the process of decomposition of ledeburite into more stable eutectic carbides begins, providing technological plasticity for subsequent forging. The influence of the purity of white cast iron on the morphology of excess carbides and their ability to divide has been established. Sukhanov D.A. also investigated [24] the morphology of excess eutectic carbides after melting, pre-annealing and after deformation forging. It is noted that the stoichiometric composition of faceted eutectic carbides is in the range of  $34 < C < 36 \text{ at.}\%$ , which corresponds to  $\text{Fe}_2\text{C}$  type  $\epsilon$ -carbide with a hexagonal close-packed lattice. A two-stage mechanism of transformation of excess secondary cementite into faceted eutectic  $\epsilon$ -carbides of the  $\text{Fe}_2\text{C}$  type during heat treatment is considered.

The study of the decay of martensite, perlite and quasi-perlite structures has been carried out in a number of works [25-29]. Pereira H.B. [28] showed that the two initial microstructures (perlite and lower bainite) were compared

in their propensity to spheroidization by dilute eutectoid transformation (DET) during the simulation of the HAZ thermal cycle. The kinetics of phase transformations in the heat treatment process was also analyzed using high-resolution dilatometric studies. The results showed that lower bainite has a greater tendency to spheroidize cementite than perlite due to the initial configuration of carbides. In addition, it has been confirmed that the higher the cooling rate, the lower the tendency to spheroidization.

Ribamar G.G. [29] using in-situ synchrotron X-ray diffraction, contact dilatometry, scanning electron microscopy, microhardness and atomic probe tomography, he found out the mechanisms of stabilization and decay of carbon in austenite of high-carbon bearing steels ( $\% C > 0.8$ ), the microstructure of which consists of solid hardened martensite (a't) + spheroidized cementite ( $\Theta\text{-Fe}_3\text{C}$ ) + a small amount of preserved austenite (yR). This complex microstructure is achieved by quenching from intercritical annealing (in the phase field cementite  $\Theta\text{-Fe}_3\text{C} + \text{yR}$ ) followed by tempering at low temperature (200-250°C). The time and temperature necessary for the effective separation of carbon into austenite or microstructural decomposition into secondary cementite have been identified.

The results obtained are discussed on the basis of various equilibrium states between martensite a't and carbides. It was found that at temperatures below 300°C, carbon stratification towards the preserved austenite occurs within a few minutes without significant phase decay. The transition temperature between the predominant enrichment of austenite with carbon and the decomposition of austenite occurs at 350°C. Secondary deposition of cementite inside martensite and at the a't/yR boundaries is observed during tempering at temperatures above 400°C. The results of carbon equilibrium modeling, taking into account the presence of carbides, show that uniformly dispersed spheroidized primary cementite has little effect on the phenomenon of carbon separation.

Carbides of the  $\text{M}_3\text{C}$  and  $\text{M}_7\text{C}_3$  type in the microstructure of white cast irons, the composition of which depends on alloying and heat treatment mode, were studied by Mikhailovich, M. [30].

The performed brief review [31-33] clearly shows that the performed studies are in the traditional paradigm defined by the Fe-C alloy state diagram, and in particular, from the concept of ledeburite as a two-phase eutectic structure consisting of cementite (iron carbide  $\Theta\text{-Fe}_3\text{C}$  containing 6.67%C) and ferrite (solid solution carbon in the  $\alpha\text{-Fe}$  polymorph). In the works of the author [31-33], a previously unknown phase transformation was discovered within the Fe-C diagram, as the peritectoid transformation of perlite into a polycarbide structure consisting primarily of monocarbide FeC and  $\epsilon$ -carbide  $\text{Fe}_2\text{C}$ .

With all the helplessness of existing chemical and industrial technologies in the field of synthesis of FeC monocarbide and obtaining it in crystalline state, the author found [30-32] that FeC monocarbide perfectly co-crystallizes in the process of peritectoid transformation [30] of lamellar eutectoid in white eutectic cast iron [31] with  $\epsilon$ -carbide  $\text{Fe}_2\text{C}$  from supersaturated solid solution based on  $\epsilon$ -carbide  $\text{Fe}_2\text{C}$  or polycarbide quasi-eutectic. In development

of the obtained new data [30-32], the author carried out additional studies of the fine structure of polycarbide quasi-eutectics.

## 2. Equipment, Materials and Research Methodology

The present investigations were carried out on two-component (Fe-C) white eutectic cast iron (C=4.3%C) of high purity, smelted in a micro-arc electric furnace according to the method [31]. Fine microstructure studies were performed on cast samples and samples that underwent prolonged isothermal annealing at  $330^{\circ}\text{C} \pm 10^{\circ}\text{C}$  for 36 h to complete the peritectoidal transformation of lamellar eutectoid (troostite) [30-32].

Metallographic studies were carried out on a Leica DMIRM digital optical metallographic microscope using Image Scope Color M image analysis software.

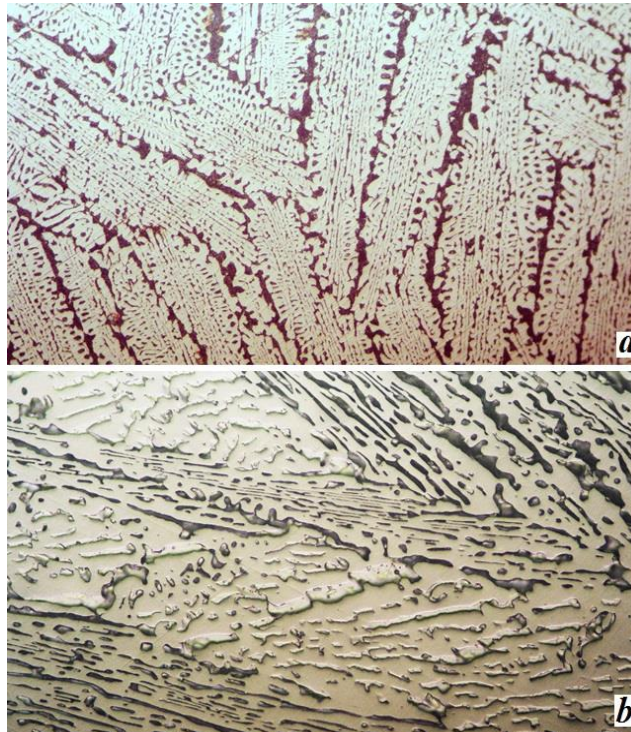
For a more detailed assessment of phase transformations and emerging structures in the process of peritectoidal transformation, the fine ledeburite structure of the lamellar eutectoid was investigated both in the cast state and after isothermal annealing using FEI Scios 2 LoVac double-beam electron microscope using DualBeam™ super-resolution analytical technology, which provides the study of fine structure in two-dimensional and three-dimensional projection. To reveal the two-dimensional surface structure of white cast iron ledeburite we used etching with 5% nitric acid solution in alcohol (Nital) at  $24^{\circ}\text{C}$  for 3-5 sec. To reveal the internal three-dimensional structure of polycarbide quasi-eutectic it was dissolved in the process of hot etching with 5% nitric acid solution in distilled water at  $50^{\circ}\text{C}$  for 5-10 sec (in some variants up to ~1.0 min) with subsequent washing of microdots in alcohol. As a result of removal of eutectoid colonies content during etching, an internal cavity or phase cell (working term) with inclusions of carbide phase is formed in the ledeburite skeleton (matrix). Chemical local microanalysis of the phases was performed using an X-ray vacuum spectrometer EDAX Octane Elite Plus, which uses a detector based on silicon nitride ( $\text{Si}_3\text{N}_4$ ), which provides a significant improvement in sensitivity to the concentration of the determined elements.

## 3. Discussion of Experimental Results

The average thickness of ferrite plates in the lamellar eutectoid of ledeburite white cast iron in the cast state (Figure 1a) varies within  $\delta_{\text{fer}}=0.095\dots 0.170\ \mu\text{m}$ , and the average thickness of cementite plates  $\delta_{\text{cem}}=0.015\dots 0.055\ \mu\text{m}$ . The degree of dispersity of the lamellar ferrite-cementite mixture is in the range  $\delta=0.110\dots 0.225\ \mu\text{m}$ , which corresponds to quasi-perlite or troostite (Figure 2a).

In the process of isothermal annealing, the peritectoidal reaction of dissolution of cementite in ferrite [30-32] with formation of supersaturated solid solution based on  $\epsilon$ -carbide  $\text{Fe}_2\text{C}$  begins to occur in the lamellar troostite of ledeburite (Figure 2a) by the reaction:  $\Theta\text{-Fe}_3\text{C}$  (cementite) +  $\alpha\text{-Fe}$  (ferrite) =  $\epsilon$ -carbide  $\text{Fe}_2\text{C}$  (supersaturated solid solution).

**Figure 1**  
Structure of lamellar eutectoid (troostite) of ledeburite in eutectic white cast iron



a - cast structure

b - after completion of peritectoid transformation during isothermal holding for 36 h at  $330^{\circ}\text{C} \pm 10^{\circ}\text{C}$ ; x500, nital etching

Upon completion of peritectoid transformation, the lamellar troostite of ledeburite white cast iron (Figure 2a) completely transforms into polycarbide quasi-eutectic (Figure 1b) based on a supersaturated solid solution of  $\epsilon$ -carbide  $\text{Fe}_2\text{C}$  [30-32], which represents a homogeneous monolithic phase with white extended inclusions of lamellar morphology (Figure 2b).

### 3.1. Morphological forms of carbide inclusions

Deep etching of polycarbide quasi-eutectic revealed a variety of morphological forms of carbide inclusions (Figure 3): globular and ellipsoidal (Figure 3a); vixers or filamentous nanocrystals (Figure 3b); lamellar (Figure 3c), which were previously revealed by surface etching (Figure 2b).

Chemical analysis showed that the globular and filamentous inclusions (Figure 3a and 3b) correspond to the chemical composition of  $\text{FeC}$  monocarbide (18.0%C) and  $\epsilon$ -carbide  $\text{Fe}_2\text{C}$  (9.6%C), while the ledeburite framework is a polycarbide quasi-eutectic including a continuous series

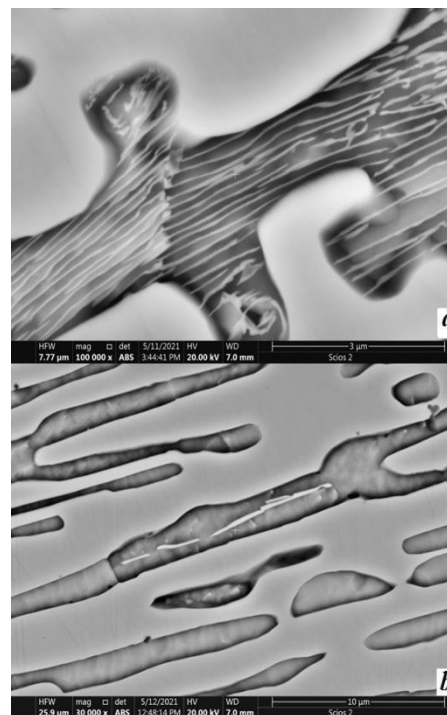
of solid solutions based on FeC carbides (18.0% C); Fe<sub>3</sub>C<sub>2</sub> (12.5% C); Fe<sub>2</sub>C (9.6% C); Fe<sub>5</sub>C<sub>2</sub> (8.0% C); Fe<sub>3</sub>C (6.67% C). Figure 4 shows the local chemical composition of carbide inclusions. The plate-like inclusions correspond to the chemical composition of  $\epsilon$ -carbide Fe<sub>2</sub>C (9.6% C). Figure 5 shows the local chemical composition of lamellar carbide inclusions.

Further investigations showed that globular and filamentous nanocrystals of carbide inclusions (Figure 3a and 3b) are nucleated crystals of FeC (18.0% C) monocarbide and  $\epsilon$ -carbide Fe<sub>2</sub>C (9.6% C), and lamellar carbide inclusions (Figure 2b and 3c) are either formed lamellar single crystals based on  $\epsilon$ -carbide Fe<sub>2</sub>C (9.6% C) or composite lamellar crystals based on co-crystallisation of  $\epsilon$ -carbide Fe<sub>2</sub>C (9.6% C) and monocarbide FeC (18.0% C).

### 3.2. Homogeneous crystallisation of single crystals of $\epsilon$ -carbide Fe<sub>2</sub>C

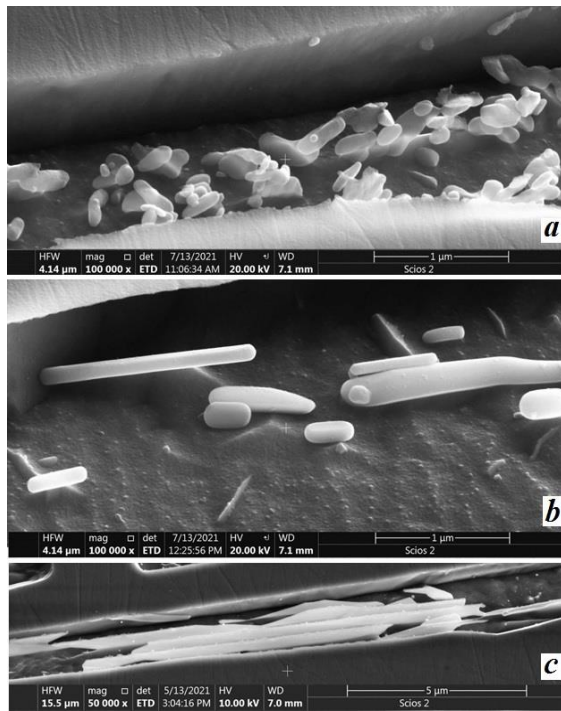
Figure 6 shows the main stages of the process of nucleation and growth of lamellar single crystals of  $\epsilon$ -carbide Fe<sub>2</sub>C on homogeneous crystallization centres (Figure 4). Nucleation starts with the formation of globular or spherical nuclei (Figure 3a and Figure 6a, item 1), with diameters from 20-40 nm, which during growth form vixers or filamentous nanocrystals (Figure 3b and Figure 6a, item 2) with diameters up to 50 nm and average lengths from 100 to 300 nm. In the process of further crystallizations, vixers aggregate into flat crystalline packages (Figure 6a, item 3), which crystallize into extended plate-like single crystals of  $\epsilon$ -carbide Fe<sub>2</sub>C (Figure 2b; Figure 3c and Figure 6b) during growth intensification. The considered growth process of single crystal of  $\epsilon$ -carbide Fe<sub>2</sub>C in the form of isolated inclusions confirms its stoichiometric composition as a chemical compound or bertollide.

**Figure 2**  
**Fine structure of ledeburite eutectoid in eutectic white cast iron**



a - cast structure of lamellar troostite in the phase cell of ledeburite framework (x100000)  
b - homogeneous monolithic structure of eutectoid colonies after completion of peritectoid transformation during isothermal holding for 36 h at 330°C ± 10°C (x30000)

**Figure 3**  
**Morphological shapes of carbide inclusions in phase cells**



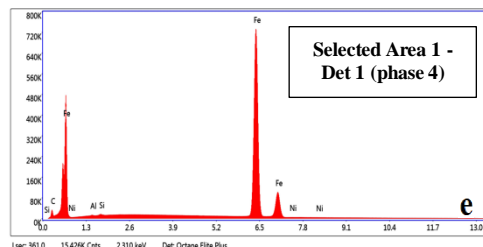
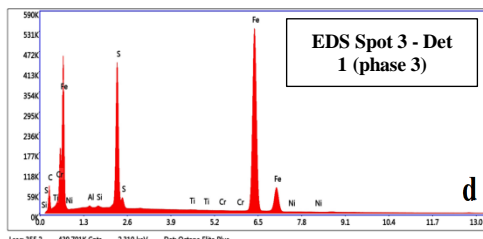
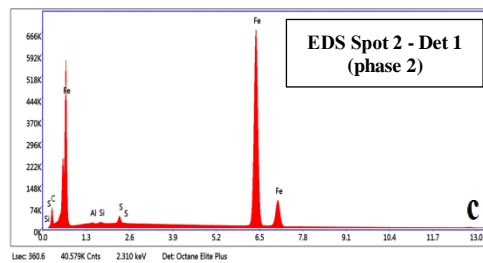
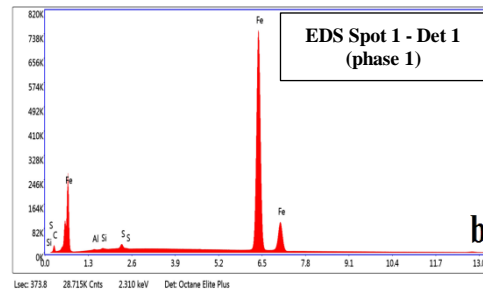
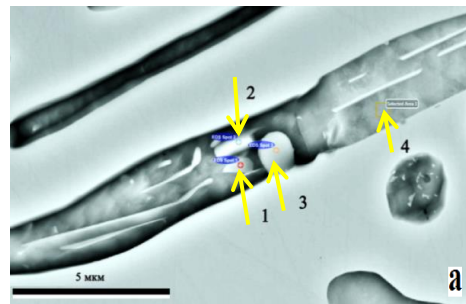
a - globular and ellipse-shaped (x100000);  
 b - vixers or filamentous nanocrystals (x100000)  
 c - lamellar (x50000)

### 3.3. Homogeneous crystallization of FeC monocarbide single crystals

Figure 7 shows the main stages of nucleation and growth of homogeneous single crystals of FeC monocarbide (Figure 4).

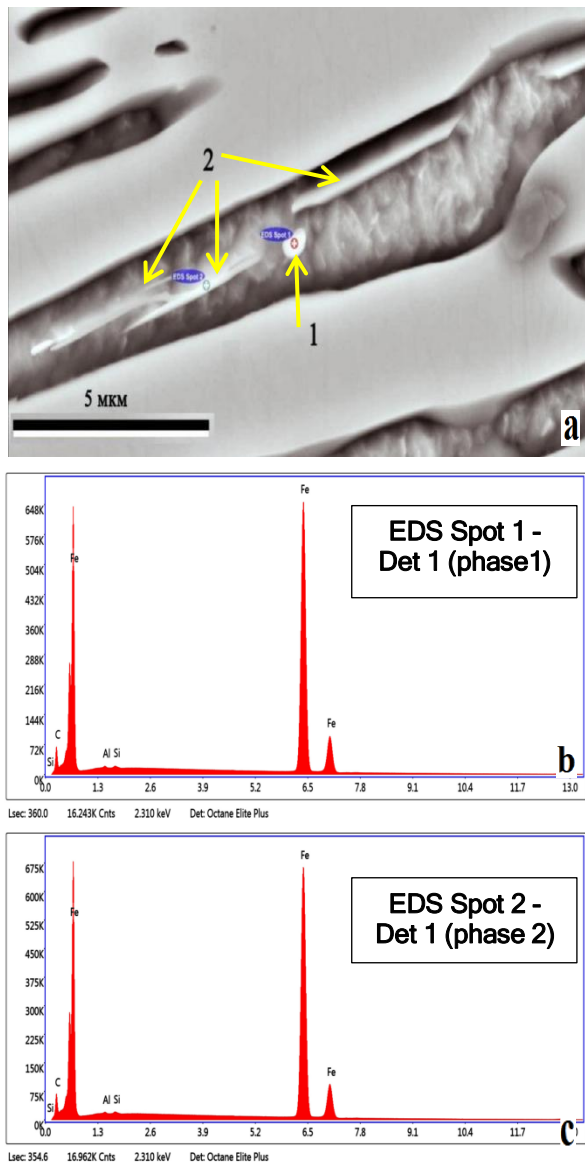
Crystallization of FeC monocarbide begins with the nucleation of spherical nuclei with diameters from 50 to 100nm (Figure 7a, item 1) on microroughnesses of the inner surface of the phase cell with subsequent growth to the inclusion of an elongated ellipsoid of rotation (Figure 7, item 2), which subsequently forms the FeC monocarbide crystal body with a smooth crystallization front (Figure 7, item 3). At further growth of FeC monocarbide monocrystal, the smooth crystallization front on its surface changes to a cellular crystallization front (Figure 7, item 4), which forms a two-dimensional crystalline nanofilm of FeC monocarbide (Figure 7, item 5). This fact is confirmed by the presence of a thin interface on the crystal surface, which is covered by the nanofilm during its movement along the crystal surface (Figure 7a, item 5, yellow arrow) and the formation of a two-layer flat crystal (Figure 7b, item 5, yellow arrow). As further growth progresses, the crystal configuration begins to acquire a distinctly dendritic structure (Figure 7b).

**Figure 4**  
 Spectral analysis of carbon content



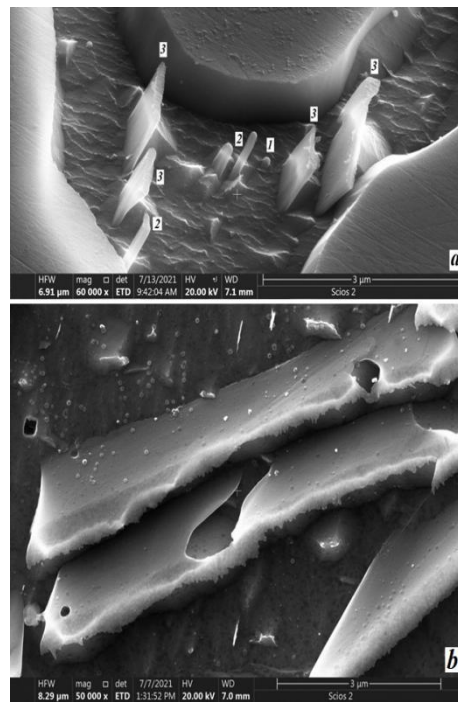
a - in globular and cylindrical carbide inclusions (phases by the yellow arrow);  
 b - 10,21%C (phase 1 Fe<sub>2</sub>C);  
 c - 11,0%C (phase 2 Fe<sub>2</sub>C)  
 d - 17,11%C (phase 3 FeC)  
 e - 7,38%C (phase 4 Fe<sub>5</sub>C<sub>2</sub>)

**Figure 5**  
 Spectral analysis of carbon content



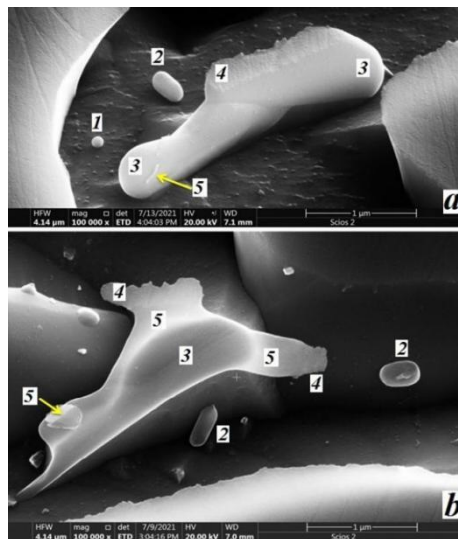
a - in globular and lamellar carbide inclusions (phases in yellow arrow);  
 b - 10,23%С (фаза 1 Fe<sub>2</sub>C);  
 c - 9,84%С (фаза 2 Fe<sub>2</sub>C)

**Figure 6**  
 Process of nucleation and growth of lamellar single crystals of ε-carbide Fe<sub>2</sub>C in phase cells



a - main stages of nucleation and growth (1-globular nucleation; 2-growth of whiskers from globular crystallization center; 3-growth of whiskers into flat crystal packages), x60000  
 b - formed extended lamellar single crystals of ε-carbide Fe<sub>2</sub>C, x50000

**Figure 7**  
 Nucleation and growth of homogeneous FeC monocarbide monocrystal



a - initial stage of FeC monocarbide crystal development (x100000)

b - cross section of FeC monocarbide crystal body with film-cellular growth surfaces (x100000);

1 - globular crystallization centre;

2 - growth of crystallization centre in the form of an elongated ellipsoid of rotation;

3 - FeC monocarbide crystal body;

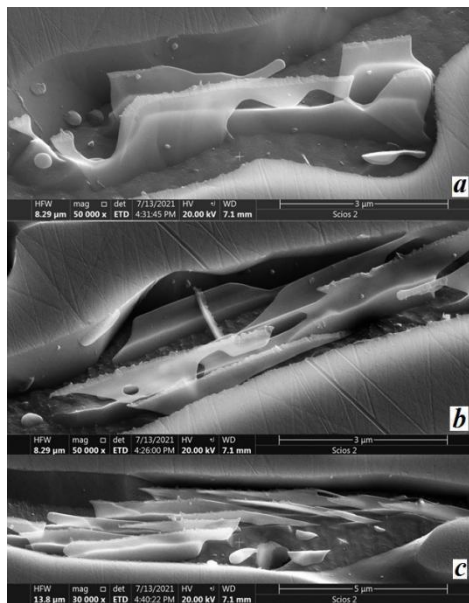
4 - cellular crystallization front;

5 - two-dimensional crystalline nanofilm of FeC monocarbide

Figure 8 shows different morphological forms of the two-dimensional crystalline FeC monocarbide nanofilm in the form of flat, extended, ribbon-shaped inclusions forming dense crystal associations. The two-dimensional crystalline nanofilm of FeC monocarbide has an incredible and unusual property - it is matte-transparent and the contours of the structures behind the nanofilm can be clearly seen through it. Moreover, it is so elastic that it envelops neighbouring carbide inclusions (Figures 8a and 8b).

The obtained experimental data fully confirm the theoretical studies of the crystallographic structure of FeC monocarbide performed by a Dong F [13,14].

**Figure 8**  
Morphological shapes of two-dimensional crystalline nanofilm of FeC monocarbide allotropes



a, b - x50000

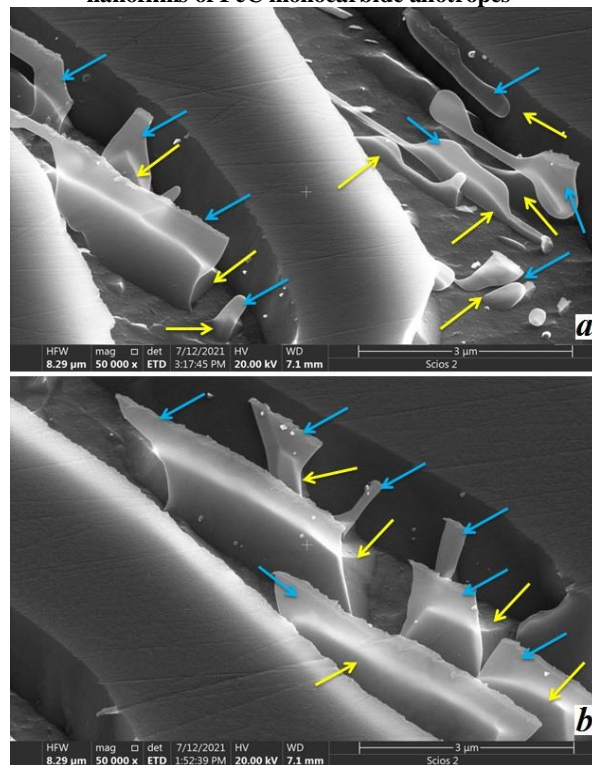
c - x30000

Using systematic ab initio calculations, they theoretically discovered energetically stable two-dimensional allotropes of FeC monocarbide characterized by planar hypercoordination chemical bonding, respectively: tetragonal FeC monocarbide (t-FeC) and orthorhombic FeC monocarbide (o-FeC). Allotropes of FeC monocarbide is the first example of 2D monolayers with

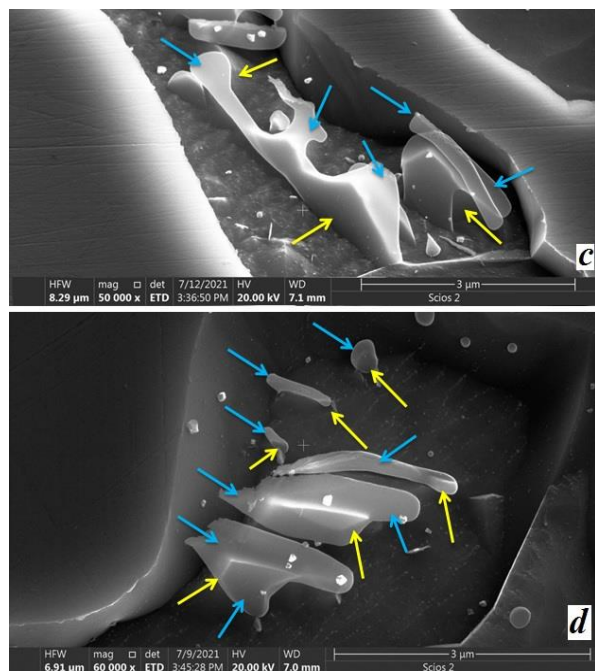
simultaneously pentacoordinated carbon bonds and seven-coordinated iron atom bonds in known iron-carbon materials.

In fact, Figure 7b and Figure 8 show the homogeneous crystallization of 2D monolayers of FeC monocarbide allotropes in the form of translucent extended and elastic crystalline nanofilms. Based on the fine structural organization of the detected nanofilms, they are completely inert to the nitric acid etching process, which indicates their high chemical resistance in addition to the results of theoretical calculations, which showed [13,14] that 2D-monolayers of FeC monocarbide allotropes have significant dynamic, mechanical and thermal stability, and, as was found experimentally above, have high elasticity or plastic properties.

**Figure 9**  
Multiple elements of heterogeneous crystallization of nanofilms of FeC monocarbide allotropes







a, b - growth of the nanofilm on the lateral surface, (x50000)  
 c, d - enveloping the surface of protruding elements, (x60000); yellow arrow - microrelief elements; blue arrow - two-dimensional crystalline nanofilm of FeC monocarbide allotropes

### 3.4. Heterogeneous crystallization of FeC monocarbide single crystals

In addition to homogeneous crystallization of 2D monolayers of FeC monocarbide allotropes on their own nuclei, heterogeneous crystallization of FeC monocarbide allotropes on the inner surfaces of phase cell microrelief elements was also found, which further confirms the truth of Dong F theoretical calculations [13,14]. Figure 9 shows multiple elements of heterogeneous crystallization of FeC monocarbide allotrope nanofilms on different surfaces of the phase cell.

In Figure 9a and 9b, the two-dimensional FeC monocarbide allotrope nanofilm crystallizes on different surfaces of protruding microroughness elements (yellow arrow - micro-relief elements; blue arrow - two-dimensional crystalline FeC monocarbide allotrope nanofilm). The FeC monocarbide allotropes nanofilm is matte-transparent and the darker elements of the microroughnesses of the carbide surface of the phase cell shine through it.

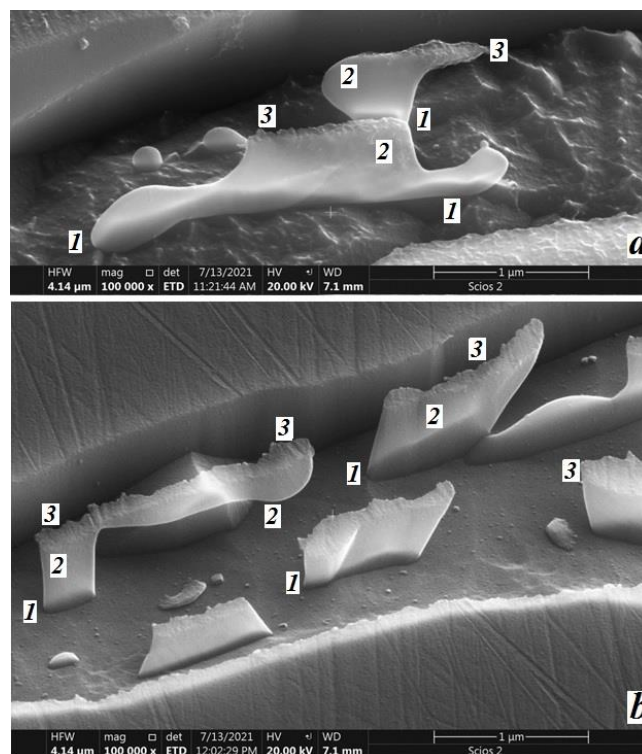
In Figure 9c and 9d, the two-dimensional FeC monocarbide allotropes nanofilm tightly envelops the surfaces of the protruding microroughness elements (yellow arrow - microrelief elements; blue arrow - FeC monocarbide two-dimensional crystalline allotropes nanofilm). The FeC monocarbide allotropes nanofilm is matte-transparent and darker elements of microroughnesses

of the carbide surface of the phase cell shine through it. It should be noted that the elasticity of the FeC monocarbide allotropes nanofilm appears only after etching, when the solid solution based on  $\epsilon$ -carbide  $\text{Fe}_2\text{C}$ , into which the nanofilm grew during its growth, is completely dissolved by nitric acid in the phase cell. Once the solid solution is removed, the nanofilm loses its stability and envelops the underlying microrelief surface of the phase cell, which can be clearly seen in Figure 9d. In Figure 9a and 9b, the upper part of the nanofilm protruding above the surface of the facet on which it grows is short and maintains its rigidity and hence its vertical position.

### 3.5. Co-crystallization of FeC monocarbide on $\epsilon$ -carbide $\text{Fe}_2\text{C}$ substrates

Figure 10 shows the co-crystallization of FeC monocarbide on  $\epsilon$ -carbide  $\text{Fe}_2\text{C}$  substrates. As established by the present studies, crystallization of the FeC monocarbide allotrope nanofilm starts either on single voxels (Figure 10a, item 1) or on lamellar packets (Figure 10b) of  $\epsilon$ -carbide  $\text{Fe}_2\text{C}$ . The FeC monocarbide allotrope nanofilm is so transparent that the  $\epsilon$ -carbide  $\text{Fe}_2\text{C}$  vixer is completely visible through the nanofilm covering it (Figure 10a, item 1).

**Figure 10**  
 Development and growth of nanofilm crystals of FeC monocarbide allotropes on  $\epsilon$ -carbide  $\text{Fe}_2\text{C}$  substrates



a - co-crystallization with vixers (x100000)  
 b - co-crystallization with plate packets (x100000);

- 1 - vixer substrate of  $\varepsilon$ -carbide  $\text{Fe}_2\text{C}$ ;
- 2 - two-dimensional crystalline nanofilm of FeC monocarbide allotropes;
- 3 - cellular crystallization front of FeC monocarbide allotropes nanofilm

Longer allotrope nanofilm of FeC monocarbide lose stability after etching and envelop the structural elements of the phase cell (Figure 10b, item 2). Shorter FeC monocarbide allotrope nanofilm retain rigidity and vertical position with a cellular crystallization front (Figure 10b, item 3).

### 3.6. Crystallization conditions of FeC monocarbide and $\varepsilon$ -carbide $\text{Fe}_2\text{C}$

The considered crystallization processes of FeC monocarbide and  $\varepsilon$ -carbide  $\text{Fe}_2\text{C}$  are determined by the following conditions.

#### 3.6.1. Dispersive solidification

After completion of peritectoid transformation [30-32], a supersaturated thermodynamically non-equilibrium solid solution based on  $\varepsilon$ -carbide  $\text{Fe}_2\text{C}$  is formed (Figure 11), which undergoes decomposition by the mechanism of dispersion solidification with the release of the phase of carbide nanocarbide nano-inclusions of FeC monocarbide and  $\varepsilon$ -carbide  $\text{Fe}_2\text{C}$  with a size range of 20-40 nm (Figure 3a).

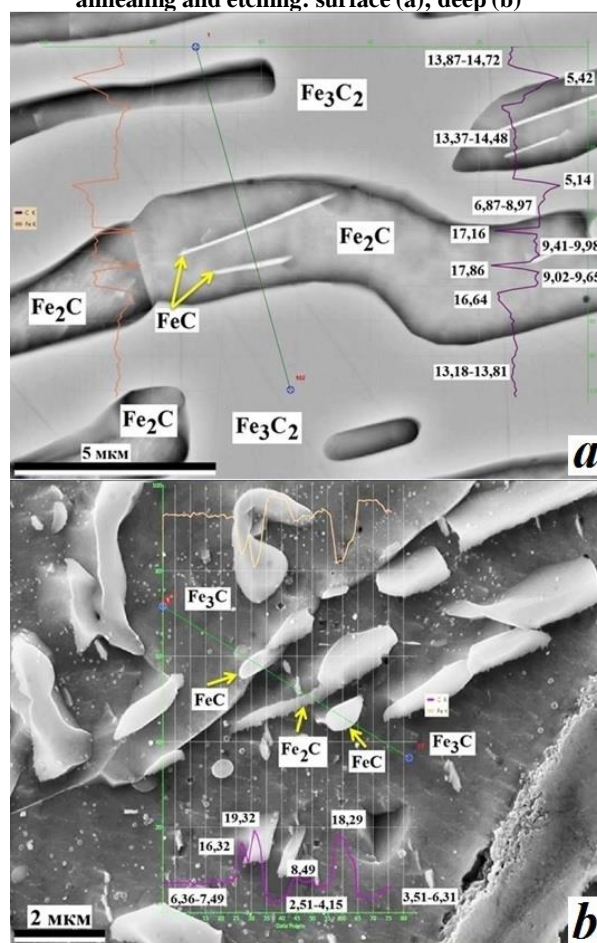
#### 3.6.2. Isovalent isomorphism

Numerous studies of the carbon content in ledeburite of white cast iron (Figures 11 and 12) have shown that its composition does not correspond to the generally accepted carbon content corresponding to cementite  $\Theta$ - $\text{Fe}_3\text{C}$  (6.67%C). Chemical composition by carbon in all carbide phases of ledeburite is gradient and varies in wide ranges, which correspond to the carbon content of the following series of carbides: FeC (18.0%C);  $\text{Fe}_3\text{C}_2$  (12.5%C);  $\text{Fe}_2\text{C}$  (9.6%C);  $\text{Fe}_7\text{C}_3$  (8.0%C);  $\text{Fe}_5\text{C}_2$  (8.0%C);  $\text{Fe}_3\text{C}$  (6.67%C);  $\text{Fe}_4\text{C}$  (5.0%C). Chemical analysis revealed the following features of carbon distribution in carbide structures of ledeburite of eutectic white cast iron after isothermal annealing. Average carbon content: in the carbide framework of ledeburite - 12,0 ... 14,0%C; on the surfaces of phase cells - minimum 3,7 ... 4,8%C, maximum 5,5 ... 8,4%C; carbide inclusions of different morphology - 15,0 ... 23,0%C (Figure 11 and Figure 12). There is a rather simple explanation for this phenomenon.

In the work of Russian scientist Barinov V.A. shown [33] that all structural models of iron-based carbide phase can be summarized in the "average" model with a finite number of iron and carbon atoms  $n_{\text{Fe}}=40$  and  $n_{\text{C}}=24$ , localized in the space group Pnma on seven and five crystallographic non-equivalent positions of the rhombic cell, respectively. For example, in such a universal cell, the cementite phase  $\Theta$ - $\text{Fe}_3\text{C}$  corresponds to 25%, and the Hegg carbide phase  $\chi$ - $\text{Fe}_5\text{C}_2$  less than 44 at.% of the maximum

allowed number of iron and carbon atoms. In the framework of this model [33], carbon atoms do not replace the iron atoms of the matrix, but are located in the gaps between them. The dissolving carbon atoms enter the gaps between the matrix iron atoms (internodes), statistically occupying a new position not previously occupied. Since with increasing carbon concentration in the alloy, the same carbon atoms with the same ionic radius and valence are added to the sub lattice of iron as a solvent without changing the electro neutrality of the crystal lattice of the solid solution, this type of isomorphism can be defined as isostructural isovalent isomorphism.

**Figure 11**  
Carbon content in the carbide phases of ledeburite after annealing and etching: surface (a); deep (b)

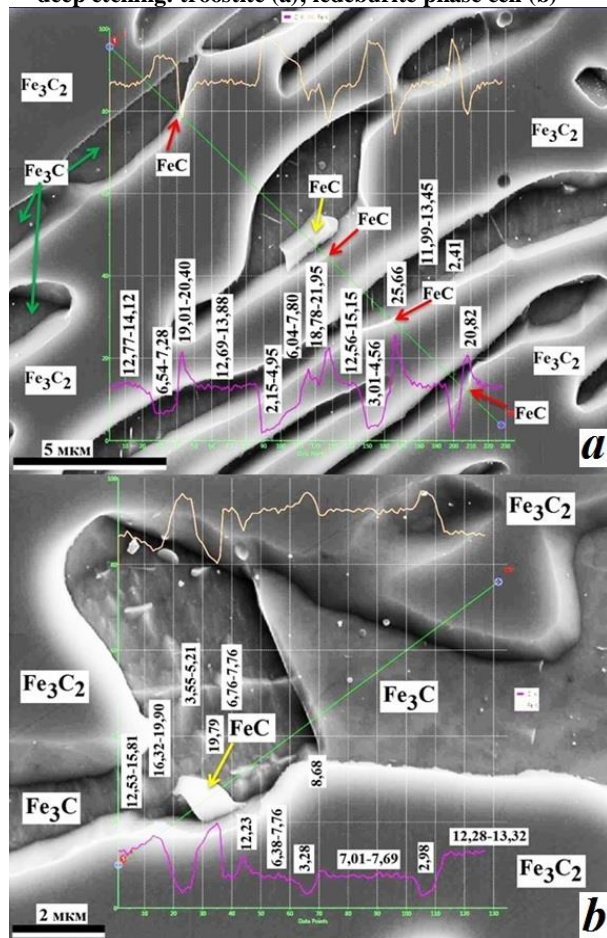


A consequence of the isostructural character of carbide phases is the universality of any carbide surface as a coherent surface for the nucleation of crystallization centers during dispersion solidification, for example, crystallization centers are formed on any carbide surface: on the phase cell surface (Figure 3a, Figure 7a), on the surface of  $\varepsilon$ -carbide  $\text{Fe}_2\text{C}$  inclusion packets (Figure 6b), on the surface of FeC monocarbide allotrope nanofilms (Figure 8a, Figure 9b).

Consequently, the carbide phases in white cast iron can be characterized as a single isomorphous and

isostructural quasi-carbide solid solution, which structurally crystallizes in the form of heterogeneous carbide phases as a quasi-eutectic [30-32], in which the carbon content is free to vary widely without identifying the carbide phases proper as chemical compounds. In general, this structural organization can be briefly characterized as a polycarbide with a gradient crystal lattice of solid solutions corresponding in carbon concentration to one or another carbide. Moreover, FeC monocarbide and  $\epsilon$ -carbide  $\text{Fe}_2\text{C}$  are chemical compounds with stoichiometric composition, since only they crystallize in the form of isolated inclusions. The other carbides are non-stoichiometric compounds. Based on the data obtained, the author has constructed a Fe-C diagram that takes into account carbide transformations to the right of the cementite line [30-32].

**Figure 12**  
**Carbon content in carbide phases after annealing and deep etching: troostite (a); ledeburite phase cell (b)**



Consideration of non-stoichiometric compounds of iron carbides as solid solutions of excess atoms of components in the basic substance [30-32] allows us to represent non-stoichiometry as the ability of crystalline compounds to dissolve their own components, i.e. iron-based carbide phases are able to dissolve carbon. Consequently, carbon should be freely redistributed within

the iron sublattice without changing the carbide's own lattice and forming one or another type of solid solution. Thus, the carbide phase is a solid solution of introduction of the second kind. This fact is proved in the studies of Russian scientists Okishev K.Y. and Mirzaev D.A. [34], as well as Medvedeva N.I. [35], in which it is shown that the redistribution of unbound carbon in the iron sublattice of carbides occurs in four types of pores: "normal" octahedral and prismatic, as well as "distorted" octahedral and prismatic. This leads to an increase in entropy and a decrease in the free energy of carbides, which is characteristic of the behavior of carbon in solid solution, which was also established by Dong Fan [13,14], whose work proved that the high adsorption capacity of the o-FeC and t-FeC allotropes also explains the high carbon content of iron carbides up to 23,0% C, which during cooling of the high-carbon carbide melt is actively adsorbed on the monolayers of the crystal lattice of crystallizing FeC monocarbide, forming high-carbon solid solutions. Dong Fan [13,14] also showed that monolayers of o-FeC and t-FeC allotropes have very high thermal stability and can maintain their structural integrity up to 2000K. The following conclusion can be drawn from the obtained data - FeC monocarbide is the most thermally stable and thermodynamically stable iron carbide from the whole known line of iron carbides.

The most significant result of the present studies is the principal possibility of developing a technology for obtaining and extracting (electrolytic dissolution) from the eutectic of white cast iron the crystalline phases of FeC monocarbide and  $\epsilon$ -carbide  $\text{Fe}_2\text{C}$  for in-depth studies, which cannot be obtained by other methods [1-15,36,37].

#### 4. Conclusion

1) The previously unknown process of homogeneous and heterogeneous crystallization of FeC iron monocarbide and its co-crystallization with  $\epsilon$ -carbide  $\text{Fe}_2\text{C}$  from a supersaturated solid solution based on  $\epsilon$ -carbide  $\text{Fe}_2\text{C}$  or polycarbide quasi-eutectic has been investigated.

2) Crystallization of 2D monolayers of FeC monocarbide allotropes in the form of translucent extended and elastic crystalline nanofilms has been experimentally proved.

3) The carbide phases in white cast iron can be characterized as a single isomorphous and isostructural quasi-carbide solid solution, which structurally crystallizes as a mixture of carbide phases as a quasi-eutectic, in which the carbon content is free to vary widely without identifying the carbide phases proper.

4) The decomposition product of the lamellar eutectoid as a result of peritectoid transformation during isothermal annealing is a polycarbide with a gradient crystal lattice of solid solutions corresponding in carbon concentration to one or another carbide.

5) Crystallization of FeC monocarbide and  $\epsilon$ -carbide  $\text{Fe}_2\text{C}$  phases in the process of dispersion solidification of solid carbide solution on the basis of  $\epsilon$ -carbide  $\text{Fe}_2\text{C}$  in the process of isothermal annealing gives a fundamental possibility to develop the technology of their extraction

(e.g. by electrolysis) from the matrix of white cast iron for in-depth studies.

6) Chemical analysis showed that globular and filamentous inclusions correspond to the chemical composition of FeC monocarbide (18.%C) and  $\epsilon$ -carbide Fe<sub>2</sub>C (9.6%C), and the ledeburite framework is a polycarbide quasi-eutectic including a continuous series of solid solutions based on carbides FeC (18.0%C); Fe<sub>3</sub>C<sub>2</sub> (12.5%C); Fe<sub>2</sub>C (9.6%C); Fe<sub>5</sub>C<sub>2</sub> (8.0%C); Fe<sub>3</sub>C (6.67%C). Plate inclusions correspond to the chemical composition of  $\epsilon$ -carbide Fe<sub>2</sub>C (9.6%C).

7) The process of nucleation and growth of lamellar  $\epsilon$ -carbide Fe<sub>2</sub>C single crystals and two-dimensional film crystals of FeC monocarbide allotropes starts with the formation of globular or spherical nuclei, with diameters from 20-40 nm, which in the process of growth form vixers or filamentous nanocrystals with diameters up to 50 nm and average lengths from 100 to 300 nm.

### Ethical Statement

This study does not contain any studies with human or animal subjects performed by the author.

### Conflicts of Interest

The author declares that he has no conflicts of interest to this work.

### Data Availability Statement

Data available on request from the corresponding author upon reasonable request.

### References

- [1] Chemical Thermodynamics. Chemical thermodynamics of iron / Robert Lemire, Donald Alan Palmer, Peter Taylor, Berner Urs, Musikas Claude, Tochiyama Osamu. – OECD Nuclea Energy Agency Date Banc, Eds., OECD Publications, Paris, France. 2013, Vol.13a. Part 1.-1126 p.
- [2] Chemical Thermodynamics. Chemical thermodynamics of iron / Robert Lemire, Donald Alan Palmer, Peter Taylor, Hartmut Schlenz. – OECD Nuclea Energy Agency Date Banc, Eds., OECD Publications, Paris, France. 2020, Vol.13b. Part 2.-921 p.
- [3] Cahn, R. W., Haasen, P. Physical Metallurgy: 4th edition. - North Holland, 1996. - 4911 p.
- [4] Laughlin, D. E., Hono C. Physical Metallurgy: 5th edition. - Elsevier, 2014. - 2960 p.
- [5] Bahgat, M. Technology of Iron Carbide Synthesis. / Mater Sci. Technol. 2006, Vol.22. Issue 03. P.423-432.
- [6] Balfour, W. J. Electronic spectroscopy of jet-cooled iron monocarbide. The  $3\Delta_i \leftarrow 3\Delta_i$  transition near 493 nm/ Balfour, W. J., Cao, J., Prasad, C. V. V., Qian, C. X. W. //The Journal of Chemical Physics. 1995. Vol.103. No.1. P.4046–4051.
- [7] Shim, I., Gingerich, K. A. All electron ab initio investigations of the electronic states of the FeC molecule //The European Physical Journal D - Atomic, Molecular and Optical Physics, 1999, Vol.7. No.2. P.163–172.
- [8] Dale J. Brugh, Michael D. Morse. Optical spectroscopy of jet-cooled FeC between 12 000 and 18 100 cm<sup>-1</sup>// The Journal of Chemical Physics. 1997. Vol.107. No.23. P.9772-9782.
- [9] Aiuchi, K., Shibuya, K. The Electronic Spectrum of Jet-Cooled FeC in the Visible Region //Journal of Molecular Spectroscopy. 2001. Vol.209. No.1. P.92-104.
- [10] Timothy C. Steimle The permanent electric dipole moments of iron monocarbide, FeC/Timothy C. Steimle, Wilton L. Virgo, and David A. Hostutler// The Journal of Chemical Physics. 2002. Vol. 117. No.4. P. 1511-1516.
- [11] Allen, M. D. The pure rotational spectrum of FeC (X<sup>3</sup>Δ<sub>i</sub>)/ M. D. Allen, C. Pesch, M. Ziurys//The Astrophysical Journal. 2009. Vol.472. No.1. P.L57-L69.
- [12] Liu, X. W. Mössbauer Spectroscopy of Iron Carbides: From Prediction to Experimental Confirmation/ Xing-Wu Liu, Shu Zhao, Yu Meng, Qing Peng, Albert K. Dearden, Chun-Fang Huo, YongYang, Yong-Wang Li, Xiao-Dong Wen //Scientific Reports. 2016. Vol.6. P. 26184-26194.
- [13] Fan, D. Two-dimensional Iron Monocarbide with Planar Hypercoordinate Iron and Carbon/ Dong Fan, Shaohua Lu, Xiaojun Hu. // Journal of Physical Chemistry C. 2018. Vol. 122. P.15118-15124.
- [14] Fan, D. Highly Stable Two-Dimensional Iron Monocarbide with Planar Hypercoordinate Moiety and Superior Li-ion Storage Performance/ Dong Fan, Chengke Chen, Shaohua Lu, Xiao Li, Meiyang Jiang, and Xiaojun Hu // ACS Applied Materials & Interfaces. American Chemical Society. 2020. Vol. 12. No. 27. P. 30297–30303.
- [15] Larionov, K.V. Theoretical study of structural, electronic and magnetic properties of new low-dimensional compounds on the basis of transition metals / Dis... k-ta phys. mat. sciences. Speciality 1.3.8 - Physics of condensed state.//Technological Institute of superhard and new carbon materials, 2022.-115 p.
- [16] Fuxing, W., Kuangdi, X. Ledeburite, Structure and Characteristic of / In: Xu, K. (eds) // The ECPH Encyclopedia of Mining and Metallurgy. Springer, Singapore. 2022.
- [17] Trepczyńska-Lent, M. Directional Solidification of Ledeburite / Archives of Foundry Engineering. 2013. Vol.13. No.3. P. 101-106.
- [18] Park, J. S., & Verhoeven, J. D. Directional solidification of white cast iron. Metallurgical and Materials Transactions. 1996. Vol.27 No.8.P. 2328–2337.
- [19] Report Title: Malleable Iron Castings Market, Global Outlook and Forecast 2023-2029. - Chemicals and Materials. 2023.-118 p.

- [20] Rubin, H., Kuangdi, X. Malleable Cast Iron / Xu, K. (eds) // The ECPH Encyclopedia of Mining and Metallurgy. Springer, Singapore. 2023.
- [21] Sukhanov, D. A., Arkhangelsky, L. B., & Plotnikova, N. V. Damascus steel ledeburite class. IOP Conference Series: Materials Science and Engineering, 4th International Conference on Competitive Materials and Technology Processes (IC-CMTP4). 2017. Vol.175. P.1-7.
- [22] Vasyunina, N. V. Ferrum extraction in cast iron via reduction smelting of red mud / N. V. Vasyunina, I. V. Dubova, K. E. Druzhinin, T. R. Gilmanshina // CIS Iron and Steel Review. 2023. Vol. 25. P. 115–121.
- [23] Sukhanov, D. A., Arkhangelsky, L. B. Formation of eutectic carbides in the structure of high-purity white cast iron in the forging process / Materials Sciences and Applications. 2017. Vol.08. No.05.P.351-360.
- [24] Sukhanov, D. A., Arkhangel'skii, L. B., Plotnikova, N. V. Mechanism of Fe<sub>2</sub>C type eutectic carbide formation within damascus steel structure / Metallurgis. 2018. Vol. 62. P. 261–269.
- [25] Santos T. Analysis of the microstructural features of phase transformation during hardening processes of 3 martensitic stainless steels/ Thiago Santos, Danièle Chaubet, Tony Da Silva Botelho, Guillaume Poize, Brigitte Bacroix // Metall. Res. Technol. 2023. Vol.120. No.117. P.1-16.
- [26] Cios, G., Winkelmann, A., Nolze, G., Tokarski, T. Mapping of lattice distortion in martensitic steel— Comparison of different evaluation methods of EBSD patterns. 2023. Vol.253 No.6.P. 113824-113830.
- [27] Pereira, H.B. Effect of pearlitic and bainitic initial microstructure on cementite spheroidization in rail steels // Henrique Boschetti Pereira, Edwan Anderson Ariza Echeverri, Dany Michell Andrade Centeno, Samuel da Silva de Souza // Journal of Materials Research and Technology. 2023. Vol.23.P. 1903-1918.
- [28] Ribamar, G.G. Austenite carbon enrichment and decomposition during quenching and tempering of high silicon high carbon bearing steel // G.G. Ribamar, J.D. Escobar, A. Kwiatkowski da Silva, N. Schell, J.A. Ávila, A.S. Nishikawa, J.P. Oliveira, H. Goldenstein // Acta materialia.2023.Vol.247. P.1-11.
- [29] Mihailović, M., Patarić, A., Jordović. B. Heat treatment featuring the key-parameters of high chromium white cast iron microstructure. Metallurgical and Materials. 2023. No.3. P.81-83.
- [30] Davydov, S.V. Low-Temperature Carbide Transformation in Pearlite of Medium-Carbon Steels // Steel in Translation. 2020. Vol. 50. No. 9. P. 639–647.
- [31] Davydov, S.V. Temperature metastable perlite in iron-carbon alloys // Steel in Translation. 2021. Vol.51. No.11. P.805-813.
- [32] Davydov, S.V. Phase equilibria in the carbide region of the iron-carbon phase diagram // Steel in Translation. 2020. Vol. 50. No. 12. P. 888–896.
- [33] Barinov, V.A. Investigation of mechanosynthesized  $\chi$ -Hagg carbide / V.A.Barinov, A.V.Protasov, V.T.Surikov // Physics of Metals and Metallurgy. 2015. Vol.116. No.8. P.835-845.
- [34] Okishev, K.Y., Mirzaev, D.A. About possible positions of carbon atoms in the lattice of cementite // Physics of Metals and Metallurgy.2003. Vol.96. No.3. P.75-78.
- [35] Medvedeva, N.I. Influence of the effects of atomic disorder and non-stoichiometry on the carbon sublattice on the zone structure of cementite Fe<sub>3</sub>C / N.I.Medvedeva, L.E.Karkina, A.L.Ivanovsky // Physics of Metals and Metallurgy.2003. Vol.96. No.5. P.16-20.
- [36] Avdeev, Y.G., Kuznetsov, Y.I. Iron oxide and oxyhydroxide phases formed on steel surfaces and their dissolution in acidic media. Review // Int. J. Corros. Scale Inhib., 2023. Vol.12. No.2. P.366–409.
- [37] Li, C.-G. First-principle study of structural, electronic and magnetic properties of (FeC)<sub>n</sub> (n = 1–8) and (FeC)<sub>8</sub>TM (TM = V, Cr, Mn and Co) clusters / Li, C.-G., Zhang, J., Zhang, W.-Q., Tang, Y.-N., Ren, B.-Z., & Hu, Y.-F // Scientific Reports, 2017. Vol. 7. No. 1. P. 17516-17526.

How to Cite: Davydov, S. V. (2024). Crystallization of FeC Iron Monocarbide During Peritectoidal Transformation of the Lamellar Eutectoid of Ledeburite White Eutectic Cast Iron. Archives of Advanced Engineering Science. <https://doi.org/10.47852/bonviewAAES42022525>